THE ASTROPHYSICAL JOURNAL, 475:134–143, 1997 January 20

AN ISOTOPE STUDY OF CARBON MONOXIDE IN THE EDGE-ON GALAXY NGC 891

SEIICHI SAKAMOTO
Nobeyama Radio Observatory, Minamimaki, Nagano 384-13, Japan; seiichi@nro.nao.ac.jp
AND
TOSHIHIRO HANDA, YOSHIAKI SOFUE, MAREKI HONMA, AND KAZUO SORAI
Institute of Astronomy, University of Tokyo, Osawa, Mitaka, Tokyo 181, Japan
Received 1996 April 15; accepted 1996 August 16

ABSTRACT

We present high-resolution simultaneous observations of the edge-on galaxy NGC 891 in ^{12}CO and ^{13}CO emissions. The molecular thin-disk component within 10.7 kpc from the galactic center was completely covered. This data set with accurate relative calibrations of intensity scale and pointing is analyzed to examine radial variation in the physical properties of the molecular gas. The total ^{13}CO/^{12}CO luminosity ratio is 1/6.6. A low ^{13}CO/^{12}CO intensity ratio of $1/(15.4 \pm 6.0)$ is observed in the nuclear disk of about 550 pc in radius. There exists a systematic gradient of the ^{13}CO/^{12}CO intensity ratio in the main galactic disk as a function of galactocentric distance: the ^{13}CO/^{12}CO intensity ratio exhibits a notable peak of $\simeq 1/4.5$ near 4 kpc, and decreases systematically outward down to $\lesssim 1/10$ at 10 kpc. The observational results are analyzed on the basis of a CO excitation analysis. The low ^{13}CO/^{12}CO intensity ratio in the nuclear disk may be attributed to a predominance of warm molecular gas ($\gtrsim 40$ K) of moderate gas density ($\sim 10^3$ cm^{-3}), while the systematic gradient of the ^{13}CO/^{12}CO intensity ratio in the main disk can be interpreted in terms of radial decrease in the dense molecular gas fraction. Since interstellar gas in the inner part of the galaxy is mostly molecular, this variation will be ascribed to compression of molecular gas with its strength dependent on galactocentric distance rather than dissociation of low-density molecular gas by UV photons from young stars in the inner part of the galaxy.

Subject headings: galaxies: individual (NGC 891) — galaxies: ISM — galaxies: structure — ISM: molecules

1. INTRODUCTION

Star formation activity in galaxies reflects the amount and the physical conditions of molecular gas. The physical conditions of molecular gas have been investigated on a galactic scale both in external galaxies (see, e.g., Rickard & Blitz 1985; Eckart et al. 1990; Wiklind et al. 1990; García-Burillo et al. 1993; Wall et al. 1993; Xie, Young, & Schloerb 1994; Aalto et al. 1995) and in the Milky Way (Solomon, Scoville, & Sanders 1979; Liszt, Burton, & Xiang 1984; Bronfman, Bitran, & Thaddeus 1988a; Liszt 1993; Handa et al. 1993; Sanders et al. 1993; Liszt 1995; Sakamoto et al. 1995, 1996a; Helfer & Blitz 1997), especially from the point of view of their radial variations and their relation to central star formation activity and structures such as spiral arms and bars. Since mapping of nearby galaxies with large millimeter-wave telescopes requires long observation time, only a partial view of the physical conditions of molecular gas in galaxies has been obtained so far. As a consequence, there is some controversy on the radial variations and the arm-interarm difference in properties of molecular gas, partly because of the intrinsic variations among galaxies and partly because some of the molecular gas excitation studies until the present suffered from large errors caused by different beam sizes, uncertain beam efficiencies, and pointing calibrations, and from small-scale fluctuations caused by limited area coverage that might blur actual global variations. Accurate and extensive measurements of line intensities in galaxies are thus needed to extract properties of molecular gas and their variation on a galactic scale.

Simultaneous ^{12}CO and ^{13}CO observations are suited to obtain well-calibrated line intensity ratios, which are indispensable in the study of the physical conditions of molecular gas. We selected as our target a nearby (8.9 Mpc; Handa et al. 1992) edge-on Sbc galaxy, NGC 891, which is known to be an analog of the Milky Way. This galaxy is seen almost perfectly edge-on ($i \simeq 89°$; Baldwin & Pooley 1973), and the full width at half-maximum thickness of the thin-disk component of this galaxy implied from aperture synthesis maps is found to be only $\sim 6''$ (Handa et al. 1992; Scoville et al. 1993). Hence virtually all molecular gas in the thin disk can be sampled by a one-dimensional strip scan with a $14''$ beam of the Nobeyama 45 m telescope. NGC 891 had been observed by several researchers in ^{12}CO emission (Solomon 1983; Sofue, Nakai, & Handa 1987; García-Burillo et al. 1992; Handa et al. 1992; Sofue & Nakai 1993; Scoville et al. 1993) for global distribution and kinematics of molecular gas. Here we conduct ^{12}CO and ^{13}CO simultaneous observations of this galaxy for a global view of the physical conditions of molecular gas and their relation to central star formation activity and galactocentric distance.

2. OBSERVATIONS AND ANALYSIS

Strip-scan observations of the edge-on galaxy NGC 891 were carried out in ^{12}CO $J = 1$–0 and ^{13}CO $J = 1$–0 emissions from 1995 January 23 to 25 and from 1996 February 23 to 29 with the Nobeyama 45 m telescope. For both observing runs, the telescope system had a half-power beamwidth of $\simeq 14''$ at the observing frequencies. The beamwidth corresponded to 650 pc at the distance of 8.9 Mpc to the galaxy estimated from an infrared Tully-Fisher relation (Handa et al. 1992).

The reference center position of the galaxy was taken at $\alpha(1950) = 2^{\rm h}19^{\rm m}24\overset{\rm s}{.}3$ and $\delta(1950) = 42°07'17''$ (Sancisi & Allen 1979), and the position angle of the major axis (X-

axis) was taken to be 23°. Here X is positive toward the northeast. We checked the position angle by a cross-scan normal to the galactic plane along $X = +90''$ at 7".5 intervals. We observed in position-switching mode with two off-source positions at offsets in azimuth of $\pm 10'$ with respect to the reference center position. We took 67 spectra in total along the major axis with spacings of 7".5 (the Nyquist sampling) from $-247''.5$ to $+247''.5$ (tangents at 10.7 kpc) in X as shown in Figure 1.

Two single-sideband SIS receivers were used simultaneously—one for ^{12}CO and another for ^{13}CO observations. The beams of the receivers had been aligned within a 2" offset. Absolute pointing of the antenna was checked every 1.5 hr using the SiO maser source W And at 43 GHz, and was measured to be accurate to 4" rms (1/3.5 of the beamwidth). The main-beam efficiency of the antenna was 45% ± 3% and 49% ± 2% for the ^{12}CO and ^{13}CO observations, respectively. With a pair of identical receivers, we could obtain a set of data with a well-calibrated *relative* intensity scale. System noise temperatures for the ^{12}CO and ^{13}CO observations were typically 1200 and 400 K, respectively. We integrated about 15 minutes per position to get an rms statistical noise level of 130 and 45 mK (km s^{-1})$^{-1/2}$ in the T_a^* scale for the ^{12}CO and ^{13}CO observations, respectively. Spectra of the ^{12}CO and ^{13}CO emission were obtained with 2048 channel acousto-optical spectrometers of 250 MHz bandwidth corresponding to a velocity coverage of 650 km s^{-1}. The tracking velocity was set to be 425 km s^{-1} for 31 positions in the northeast part of the galaxy and 525 km s^{-1} for the other 36 positions. Baseline ranges were set to be 200–250 and 800–850 km s^{-1} for the central five positions, 200–250 and 525–575 km s^{-1} for the northeastern 31 positions, and 475–525 and 800–850 km s^{-1} for the southwestern 31 positions. Only linear baselines were subtracted from the spectra.

In order to avoid calibration and pointing error problems, the data were reduced with the following criteria in mind: If any of the ^{12}CO and ^{13}CO spectra obtained simultaneously at the same position needed to be flagged, both spectra should be discarded. This is because relative pointing calibration was established to an accuracy of the beam squint only for a set of spectra simultaneously obtained. Careful inspection of the data, however, proved that no flagging was actually needed for our data. We integrated each run with equal weighting. These procedures ensured the high accuracy of the relative calibrations in intensity scale and pointing.

Radial distance from the galactic center was derived from the velocity assuming a completely flat rotation curve at 225 km s^{-1} in a perfectly edge-on disk. Its systematic LSR velocity was assumed to be 525 km s^{-1}. We neglected the effect of velocity dispersion of molecular clouds. To avoid the effects of noncircular motion and blending of velocity components on extracted average gas properties in each radius, we limited our analysis to regions farther outer than 2.5 kpc. Properties of molecular gas near the nucleus are separately discussed.

3. RESULTS

In Figure 2 we present the total velocity profiles obtained by averaging the spectra along the major axis from $-247''.5$ to $+247''.5$ in X. Levels outside the baseline range of each profile were set to be zero. We limited our averaging range to components within 10 kpc from the center to minimize the baseline error. The luminosities of the ^{12}CO and ^{13}CO emissions integrated for all components within 10 kpc from the center were 2.9×10^8 and 4.4×10^7 K km s^{-1} pc^2, respectively. The ^{12}CO luminosity is smaller than that estimated for the entire galaxy (6.6×10^8 K km s^{-1} pc^2; Sofue & Nakai 1993). This discrepancy may be due in part to the thick-disk component, unobserved in the present work. For galaxies with metal abundances similar to those in the Milky Way, the Galactic standard CO-to-H_2 conversion factors may be safely adopted (Sakamoto 1996). Using the standard conversion factor in the Milky Way $N(H_2)/W(^{12}CO) = 2.3 \times 10^{20}$ cm^{-2} (K km s^{-1})$^{-1}$ (Strong et al. 1988), we estimate the molecular gas mass of the thin-disk component in NGC 891 to be $1.4 \times 10^9\ M_\odot$ (helium included). This value is comparable to that of the Milky Way [(1.7–2.2) $\times 10^9\ M_\odot$, adapted from Dame 1993 with a factor of 1.3 correction for helium]. The ^{13}CO/^{12}CO luminosity ratio in this galaxy was 1/6.6. This luminosity ratio is very close to that observed in the molecular gas in the inner Galaxy ($\sim$1/5.5, Solomon et al. 1979; $\simeq$1/6.7, Polk et al. 1988; $\sim$1/5, Bronfman et al. 1988a). Molecular gas in NGC 891 is thus comparable to that in the Milky Way with respect not only to the total amount but also to global physical properties.

The ^{12}CO profile shows double peaks typical of rotating disks, as Sofue & Nakai (1993) noted earlier. The ^{13}CO emission exhibits an additional central peak near its systemic velocity. The intensity of the blueshifted (or northeastern) side is less than that of the redshifted (or southwestern) side in ^{12}CO, while the opposite occurs for ^{13}CO. Molecular gas in the northeastern part of the galaxy exhibits a lower value of the ^{13}CO/^{12}CO ratio (1/7.5) than in the southwest (1/4.9). The half-maximum velocity widths of the averaged spectra were about 460 ± 5 in ^{12}CO $J = 1$–0 and about 450 ± 10 km s^{-1} in ^{13}CO $J = 1$–0. The ^{12}CO width agrees with that obtained by Sofue & Nakai

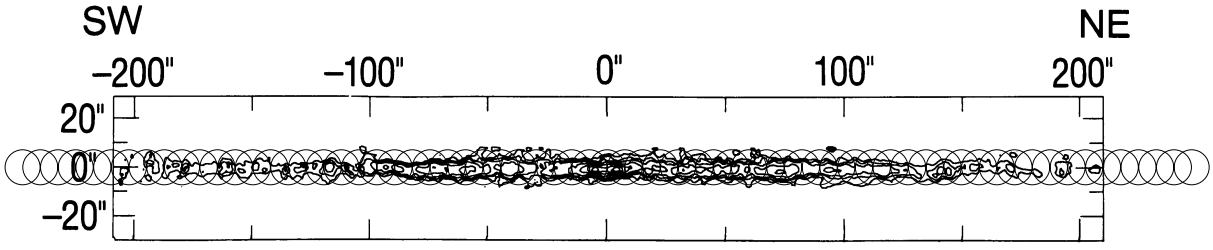

FIG. 1.—Positions of the observed points overlaid on the ^{12}CO synthesis map of Scoville et al. (1993). The size of the open circles indicates the half-power beamwidth of the 45 m antenna at 110 GHz (14"). Emission from the thin-disk component within 10.7 kpc from the center was completely covered.

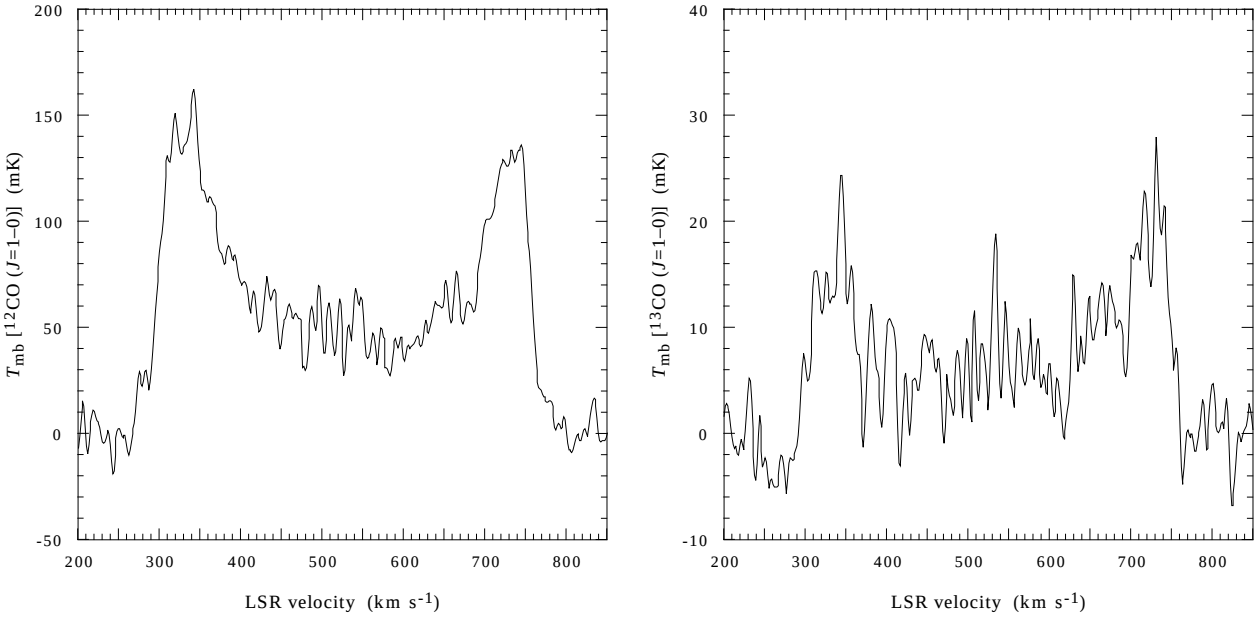

FIG. 2.—Total velocity profiles of (*left*) ^{12}CO $J = 1$–0 and (*right*) ^{13}CO $J = 1$–0 emissions averaged over $-247\farcs5 \leq X \leq +247\farcs5$

(1993) within the errors. The line width obtained for ^{13}CO observations may be narrower because the ^{13}CO emission is less affected by cloud overlapping. In the ^{12}CO profile, higher velocity components associated with the nuclear disk are visible at a 15% intensity level with respect to the peak.

Figures 3 and 4 are position-velocity diagrams of the ^{12}CO and ^{13}CO emissions, respectively, smoothed to a velocity resolution of 5 km s^{-1}. The intensities have been corrected for atmospheric attenuation and beam efficiency. The gray-scale coding was set so that emission features with a ^{13}CO/^{12}CO ratio of 1/5 appear with the same coding in both figures. The ^{12}CO emission distribution shown in Figure 3 is typical of rotating disks with surface brightness decreasing outward, but it also exhibits some peculiar features summarized below:

1. There is nuclear emission within a radius of about 550 pc, which we hereafter refer to as the "nuclear disk." It appears in the velocity range from 250 to 800 km s^{-1}, larger than the terminal velocities of the disk component by about 50 km s^{-1}. Its velocity gradient is 0.50 km s^{-1} pc^{-1}.

2. Inside the nuclear disk there are intense emission features limited by two maxima of emission near (X, v_{LSR}) = (+0.″2, 500) and (−0.″2, 550) typical of rings or bars contained in the nuclear disk. This feature has also been noted by García-Burillo & Guélin (1995) in their CO $J = 2$–1 position-velocity map. Our high-resolution data show that this feature is also visible in the CO $J = 1$–0 emission.

3. Faint emission can be seen outside the nuclear emission up to about 3 kpc from the nucleus. It is more conspicuous in the northeastern side of the galaxy.

4. In the galactic disk from 3 to 10 kpc in galactocentric distance, which we hereafter call the "main disk," intense emission is observed at about 0.1 K or more. This main-disk emission is asymmetric with respect to the center. In the northeastern side, emission is conspicuous near 3 and 8 kpc from the center, whereas intense emission is confined to the inner edge of the disk near 3 kpc in the southwestern side. The northeastern part of the galaxy is brighter in ^{12}CO.

5. Three bright complexes are seen near (X, v_{LSR}) = (+2.″4, 310), (+2.″4, 340), and (−3.″1, 730).

6. We detected the ^{12}CO emission as far as 15 kpc from the center with our 260 mK (km s^{-1})$^{-1/2}$ sensitivity in the T_{mb} scale.

The distribution of the ^{13}CO emission in Figure 4 mimics that of the ^{12}CO emission, except for the following:

1. The ^{13}CO emission is generally weaker by a factor of $\simeq 7$ as a whole.

2. There is little emission inside 3 kpc from the center including the nuclear disk emission. The ^{13}CO/^{12}CO ratio ($\equiv R_{13/12}$) is 1/(15.4 ± 6.0) in the nuclear disk (integrated for $0 \leq X \leq 22\farcs5$, $v_{LSR} = 250$–450 km s^{-1}, and $-22\farcs5 \leq X \leq 0$, $v_{LSR} = 600$–800 km s^{-1}). Although the ratio toward the nuclear disk contains large errors due to the baseline uncertainties, this ratio is significantly lower than that observed near 4 kpc from the galactic center.

3. Asymmetry of the distribution of the main-disk emission is larger in the ^{13}CO emission. Intense emission is observed along the inner edge of the main-disk component in the southwest, whereas the corresponding feature can hardly be recognized in the northeast. The southwestern part of the galaxy is brighter in ^{13}CO than the northeast.

4. The distribution of the ^{13}CO emission in the main disk is more patchy. For example, discrete complexes are conspicuous near (X, v_{LSR}) = (+2.′0, 315), (+1.′3, 340), and (−3.′0, 730).

5. No significant ^{13}CO emission was detected outside 10 kpc with our detection limit of 90 mK (km s^{-1})$^{-1/2}$ in the T_{mb} scale.

The difference in distributions of the ^{12}CO and ^{13}CO emission becomes clearer when we take the ^{13}CO/^{12}CO ratio. The asymmetric and patchy distribution of the regions with high $R_{13/12}$ mentioned above are readily seen in a position-velocity diagram of $R_{13/12}$ in Figure 5. Note that the average value of $R_{13/12}$, the missing nuclear ^{13}CO emission, and the radial decrease in $R_{13/12}$ agree well with the values obtained through large-scale observations of the Milky Way (Solomon et al. 1979; Liszt et al. 1984; Bronfman et al. 1988a).

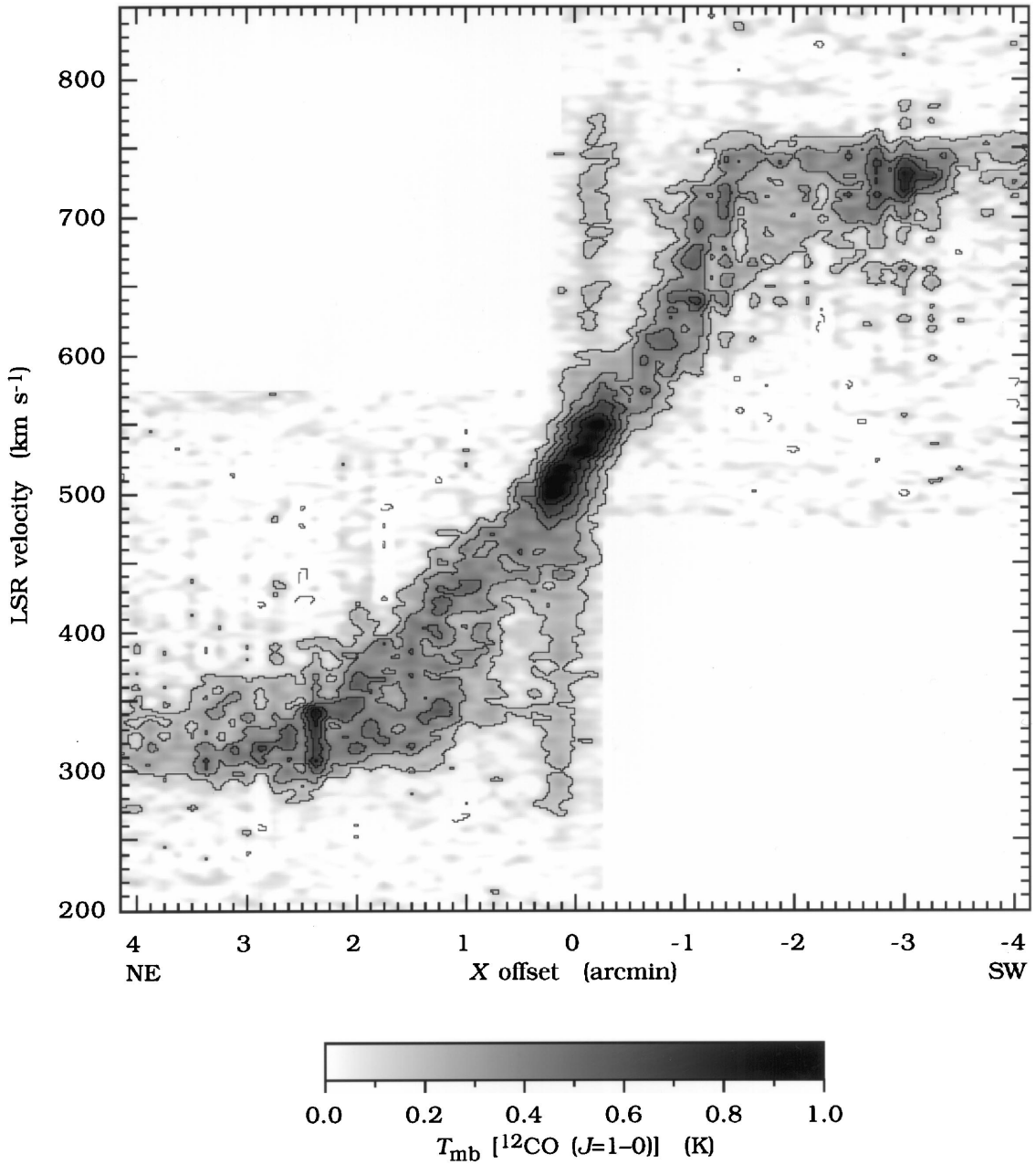

FIG. 3.—Position-velocity diagram of ^{12}CO $J = 1$–0 emission along the major axis corrected for the atmospheric attenuation and the main-beam efficiency. Spectra were smoothed to have a velocity resolution of 5 km s^{-1}. The contour interval is 0.15 K. Negative levels are indicated by dashed contours.

4. RADIAL DISTRIBUTION OF MOLECULAR GAS

Here we extract the amount and properties of molecular gas using volume emissivities after Sakamoto et al. (1996a) without identifying individual clouds or cloud associations. Volume emissivity ϵ is defined as luminosity emitted per unit volume. We binned the galactic disk in concentric annuli of width $\Delta r = 500$ pc. The volume emissivity of CO in a concentric ring with inner and outer boundaries of radii r_1 and $r_1 + \Delta r$ is given here as

$$\epsilon\left(r_1 + \frac{1}{2}\Delta r\right) \equiv \frac{D^2 \int\int_{r=r_1}^{r_1+\Delta r} T_{\rm CO}\, dv\, d\Omega}{D^2 \int\int_{r=r_1}^{r_1+\Delta r} (2\, dl/dv) dv\, d\Omega} = \frac{\sum_{\rm profiles}^{r=r_1 \to r_1+\Delta r} T_{\rm CO}}{\sum_{\rm profiles}^{r=r_1 \to r_1+\Delta r} (2\Delta l/\Delta v)}, \quad (1)$$

where D is the distance to the galaxy, l is the length of the line of sight across the ring, and Ω is a solid angle. Units of the emissivity are K km s^{-1}. The volume emissivity of the ^{12}CO $J = 1$–0 emission is a good indicator of the total amount of molecular gas, while the ^{13}CO/^{12}CO $J = 1$–0 emissivity ratio is an indicator of average properties of molecular gas. The merit of this method is that it is free from systematic omission of faint components.

Volume emissivities of the ^{12}CO $J = 1$–0 and ^{13}CO $J = 1$–0 emissions are plotted in Figure 6 as functions of the galactocentric distance calculated on completely circular and flat rotation at a velocity of 225 km s^{-1}. The obtained radial distribution of the ^{12}CO emissivity is remarkably similar to that in the Milky Way (e.g., Sanders, Solomon, & Scoville 1984; Bronfman et al. 1988b), as was noted earlier

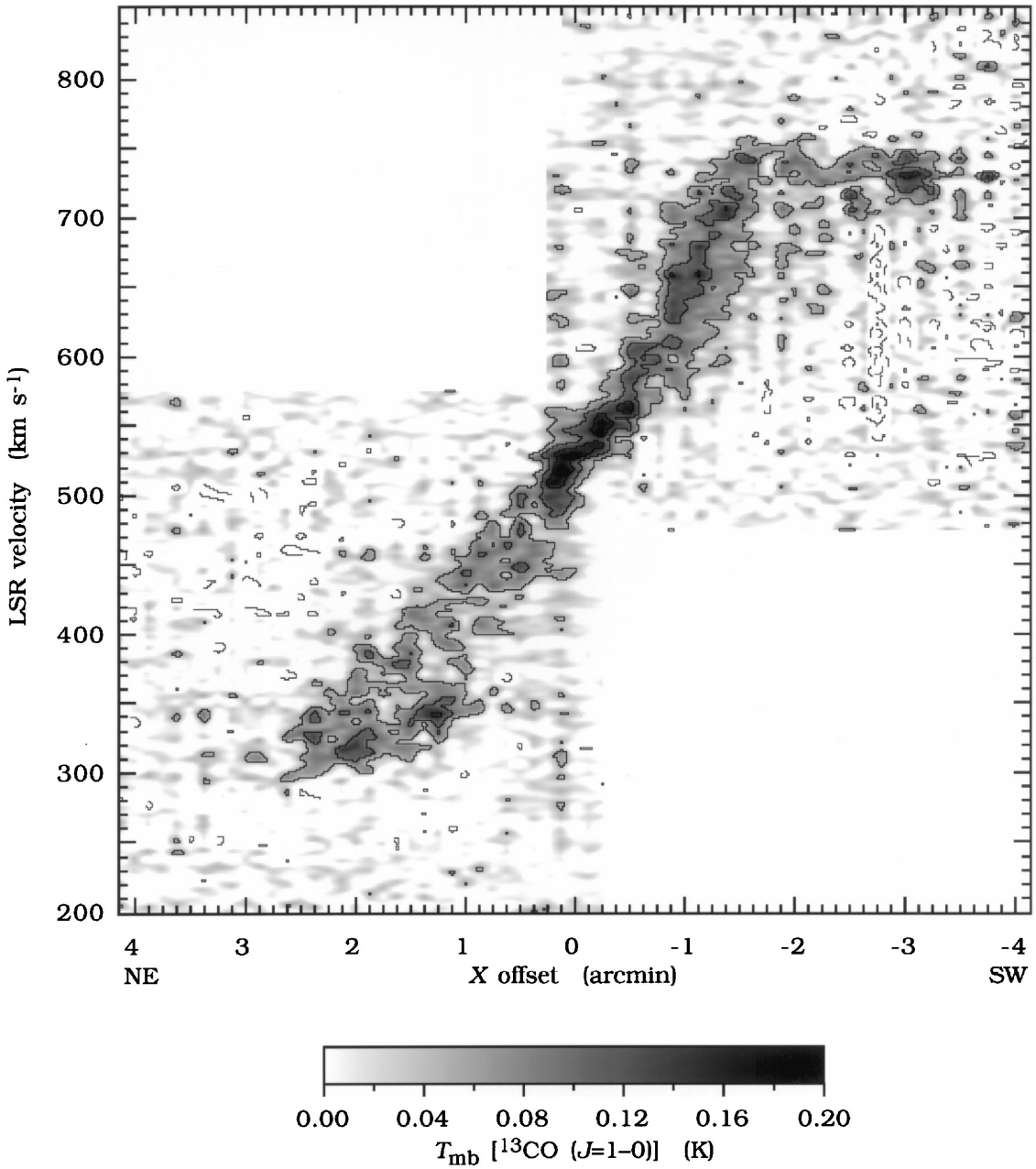

FIG. 4.—Same as Fig. 3, but for the ^{13}CO $J = 1$–0 emission. The contour interval is 0.05 K. Negative levels are indicated by dashed contours.

by Sofue & Nakai (1993) and Scoville et al. (1993): a central peak within 550 pc from the center corresponding to the nuclear disk emission, and molecular ring emission with its maximum near 4 kpc. The *e*-folding scale lengths of the main-disk component fit from 4.0 to 12.0 kpc were 3.0 kpc for the ^{12}CO emission and 1.8 kpc for the ^{13}CO emission.

5. PROPERTIES OF MOLECULAR GAS

5.1. *Meaning of the* ^{13}CO/^{12}CO *Intensity Ratio*

There exists a large-scale variation in the ^{13}CO/^{12}CO intensity ratio as a function of the galactocentric distance, as we see in Figure 6. The ratio is low ($\simeq 1/15$) in the nuclear disk, having a higher value of $\simeq 1/4.5$ in the molecular ring near 4 kpc from the center. In the outer part of the galaxy the ratio seems to be lower than 1/10. We may study global conditions of molecular gas in individual regions from the ^{13}CO/^{12}CO intensity ratio through an excitation analysis.

Up to now, extragalactic studies on properties of molecular gas have mostly been done on the basis of either simple LTE analysis or more sophisticated LVG analysis, provided that molecular gas within the beam is uniform in physical conditions or is one-zoned. The assumption of uniform physical conditions would be invalid because physical conditions of molecular gas are known to vary largely within a cloud (see, e.g., Sakamoto et al. 1994) and from one cloud to another (see, e.g., Polk et al. 1988). In this subsection we try to establish a more realistic two-zone model for extragalactic works with the aid of ^{12}CO and ^{13}CO observations of nearby molecular clouds, after a basic analysis on a one-zone model.

5.1.1. *One-Zone, One-Component Model*

A ratio of line intensities reflects differences in the lines' excitation temperatures and opacities. For molecular gas

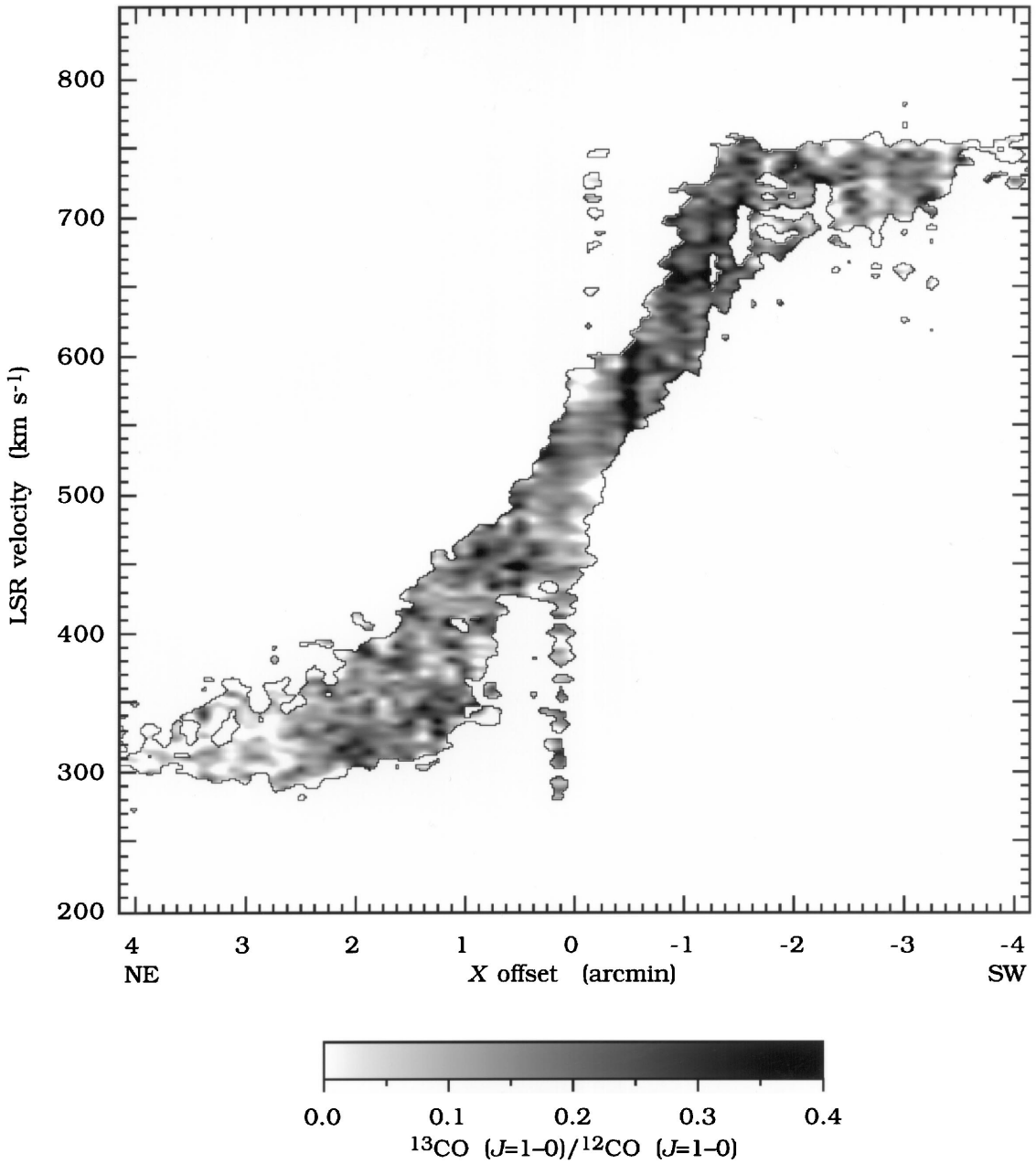

FIG. 5.—Position-velocity diagram of the $^{13}CO/^{12}CO$ intensity ratio along the major axis at a velocity resolution of 5 km s^{-1}. The ratio was calculated only for those regions with $T_{mb}(^{12}CO) > 0.2$ K. Effects of the atmospheric attenuation and the main-beam efficiency have been corrected.

whose gas density is comparable to or lower than the critical density of the emission [$n(H_2) \lesssim 10^3$ cm^{-3} for CO], collisional excitation is not sufficient to realize the LTE condition, and the photon trapping effect plays an important role in the excitation of the emission. Lines of rarer isotopes experience smaller effects of the photon trapping, resulting in lower excitation temperatures. The ^{13}CO emission may have not only smaller opacity but also lower excitation temperature than the ^{12}CO emission. Possible mechanisms that decrease the $^{13}CO/^{12}CO$ intensity ratio include (1) decrease in gas density, which introduces the non-LTE excitation and also results in lower opacity of the CO lines; (2) increase in gas kinetic temperature, which lowers the opacity of the CO lines; (3) increase in the velocity gradient of molecular clouds, which also results in lower opacity of the CO lines; (4) decrease in the CO/H_2 abundance ratio, which results in lower opacity of the CO lines; and (5) decrease in the $^{13}CO/^{12}CO$ abundance ratio, which enlarges the differences of these isotopic lines in their opacities and excitation temperatures.

Let us examine the dependence of the $^{13}CO/^{12}CO$ intensity ratio on physical conditions of molecular gas first. It is often claimed on the basis of the LTE analysis that the $^{13}CO/^{12}CO$ intensity ratio is a probe of the opacity of the ^{12}CO emission—in other words, of the column density or sizes of molecular clouds. This interpretation may not be valid in extragalactic studies because the LTE condition is rarely satisfied on scales larger than molecular clouds. Even dense molecular clouds may be surrounded by diffuse molecular gas for which the LTE analysis is not adoptable. An LVG analysis was carried out in the manner described in Sakamoto et al. (1994). Figure 7*a* shows dependence of $R_{13/12}$ on molecular gas density for different values of kinetic temperature. Increase in the kinetic temperature of

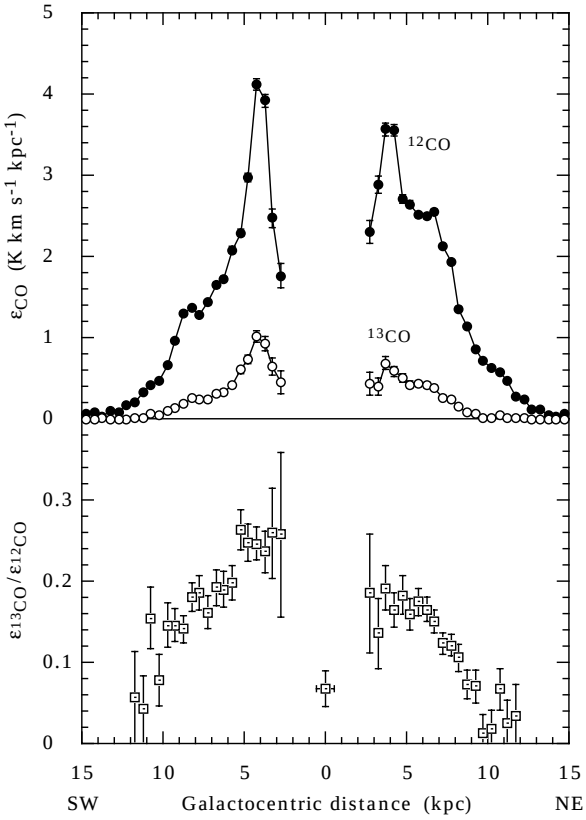

FIG. 6.—Volume emissivities of ^{12}CO $J = 1$–0 and ^{13}CO $J = 1$–0 emissions and their ratio as functions of galactocentric distance. Emissivities were calculated separately for the northeastern and southwestern sides of the galaxy. Units of the volume emissivities are K km s^{-1} kpc^{-1}. Error bars represent 1 σ errors chiefly due to the baselines at a level of 15 mK for both ^{12}CO and ^{13}CO emissions.

molecular gas can induce low $R_{13/12}$. It is, however, unlikely to be the reason for the decrease of $R_{13/12}$ from 4 to 10 kpc because we expect lower kinetic temperature as we go farther out from the galactic center. Decrease in gas density also induces low $R_{13/12}$. With the typical values of kinetic temperature, velocity gradient, and the CO abundances, the ^{13}CO/^{12}CO ratio suddenly drops down when gas density becomes less than 10^3–10^4 cm^{-3}, as Figures 7*a* and 7*b* illustrate. Since a substantial fraction of the molecular gas mass in the Milky Way is contained in the form of low-density gas that emits subthermally excited CO lines, the value $R_{13/12}$ is a probe of gas density. The velocity gradient of a molecular cloud may not change by a factor of a few or larger if molecular clouds are bound systems.

Next we examine to what extent variations in the abundance ratios affect the ^{13}CO/^{12}CO intensity ratio. Possible mechanisms that change the abundance ratio are listed in Casoli, Dupraz, & Combes (1992). These include a selective photodissociation of ^{13}CO, a chemical fractionation, a selective nucleosynthesis of ^{12}C by star formation strongly biased toward high-mass stars, and an infall of ^{13}C-deficient gas. Figure 7*b* shows the dependence of $R_{13/12}$ on molecular gas density for different values of the ^{13}CO/^{12}CO isotope ratio and the CO/H_2 abundance per unit velocity width. The ^{13}CO/^{12}CO isotope ratio in the Milky Way is expressed with the Galactocentric radius r_{GC} as $^{13}\mathrm{CO}/^{12}\mathrm{CO} = [(7.5 \pm 1.9)r_{GC} + 7.6 \pm 12.9]^{-1}$ (Wilson & Rood 1994). Provided that this relation also applies to NGC 891, the expected variation in the abundance ratio from 4 to 10 kpc is only a factor of 2.2. The possible variation in the ^{13}CO/^{12}CO isotope ratio may account for *at most* a factor of 2.2 inward increase, and probably much less. Inward increase in the CO/H_2 abundance ratio by a factor of a few may also have insignificant effects on $R_{13/12}$ unless diffuse molecular gas dominates the CO emission. To summarize, reasonable variations in the ^{13}CO/^{12}CO isotope ratio and in the CO/H_2 abundance ratio will not induce variation in $R_{13/12}$ by a factor of a few or larger.

It is possible to qualitatively diagnose kinetic temperature and gas density from $R_{13/12}$ with the aid of the $J = 2$–1/$J = 1$–0 intensity ratio $R_{2-1/1-0}$. As demonstrated in Figures 7*c* and 7*d*, $R_{2-1/1-0}$ decreases as gas density decreases in the same sense as $R_{13/12}$, while $R_{2-1/1-0}$ decreases as kinetic temperature decreases, in the opposite sense to $R_{13/12}$. We may thus simply say that those regions with low $R_{13/12}$ and low $R_{2-1/1-0}$ are dominated by emission from low-density molecular gas, and that those with low $R_{13/12}$ and high $R_{2-1/1-0}$ are dominated by emission from warm molecular gas.

5.1.2. *Two-Component Model: Lessons from Nearby Clouds*

The one-zone, one-component model analysis conducted above is an oversimplification when we apply it to the CO emission observed in external galaxies, because individual molecular clouds are not resolved in most of the external galaxies. To extract physical conditions of molecular gas properly from the ^{13}CO/^{12}CO intensity ratio, we should achieve a view of how molecular clouds would be seen as a whole in the ^{12}CO and ^{13}CO emissions.

A view of the internal structure of molecular clouds was provided from large-scale observations of nearby molecular clouds. According to the strip observations of the Orion A and B giant molecular clouds in $J = 2$–1 emissions of ^{12}CO and ^{13}CO by Sakamoto et al. (1994), there is a parsec-scale variation of $R_{13/12}$ in the clouds: the value $R_{13/12}$ is $\simeq 1/3$ in central ridges of the clouds and $\lesssim 1/20$ in their peripheries. Extensive high-resolution observations of giant molecular clouds in ^{12}CO emission revealed that there are two distinct populations of molecular gas, namely, clumps and extended tenuous components (Blitz & Stark 1986; Sakamoto et al. 1996b). Since results of the excitation analysis displayed in Figure 7 imply that the ^{13}CO emission suddenly disappears when the molecular gas density becomes less than 10^3–10^4 cm^{-3} for typical clouds with $Z(^{12}\mathrm{CO})/(dv/dr) \sim 10^{-4}$ (km s^{-1} pc^{-1})$^{-1}$, molecular gas would be better separated into two components, i.e., dense gas [$n(H_2) \gtrsim 1 \times 10^3$ cm^{-3}] with high $R_{13/12}$ ($\sim 1/3$) and tenuous gas [$n(H_2) \lesssim 2 \times 10^2$ cm^{-3}] with low $R_{13/12}$ ($\sim 1/20$), based on the observations of the Orion clouds presented by Sakamoto et al. (1994).

The value $R_{13/12}$ obtained after averaging over scales larger than typical sizes of molecular clouds would thus be better interpreted as a probe of the mixing ratio of dense molecular gas with $R_{13/12}$ of $\simeq 1/3$ and tenuous molecular gas with very low $R_{13/12}$ of $\simeq 1/20$ rather than as a probe of the optical depth of molecular gas. Similar arguments have already been given by Polk et al. (1988) and Aalto et al. (1995). Through an LVG analysis of the multiline observations of a few selected positions in this galaxy, García-Burillo et al. (1992) pointed out that at least two components—dense cores and diffuse envelopes—are needed to explain the observed CO line intensities. Recent analysis of ^{12}CO and ^{13}CO emissions from the inner

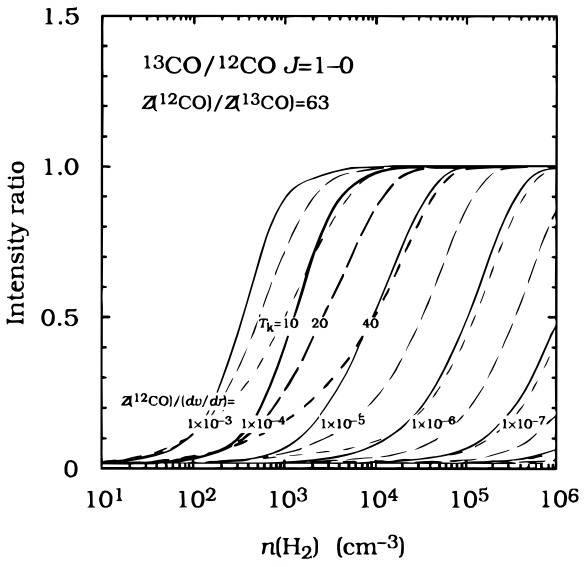

FIG. 7a

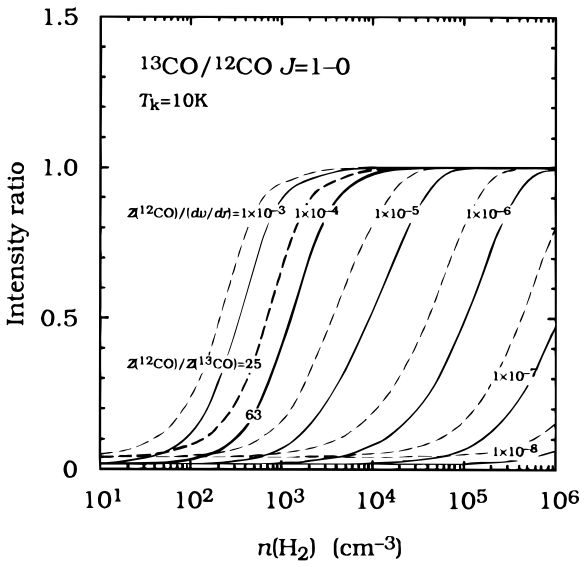

FIG. 7b

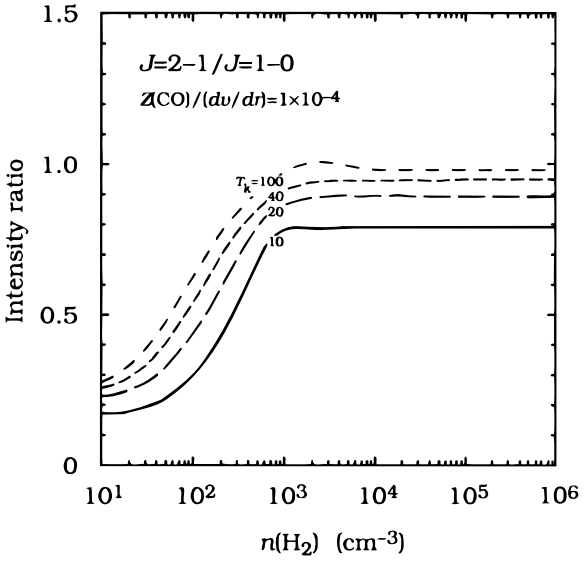

FIG. 7c

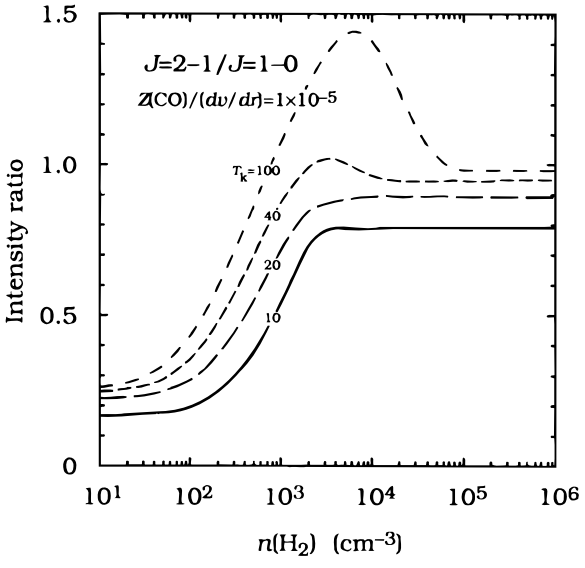

FIG. 7d

FIG. 7.—(*a*) Dependence of $^{12}CO/^{13}CO$ intensity ratio $R_{13/12}$ on molecular gas density for different values of kinetic temperature. The isotope ratio $Z(^{12}CO)/Z(^{13}CO)$ was assumed to be 63. Curves for a typical value of ^{12}CO abundance per unit velocity width $Z(^{12}CO)/(dv/dr)$ in the solar vicinity, 10^{-4} (km s^{-1} pc^{-1})$^{-1}$, are plotted in thick lines. (*b*) Same as (*a*), but for different values of $Z(^{12}CO)/Z(^{13}CO)$ and $Z(^{12}CO)/(dv/dr)$. The kinetic temperature was set to be 10 K. (*c*) Dependence of $J = 2$–$1/J = 1$–0 intensity ratio $R_{2-1/1-0}$ on molecular gas density for different values of the kinetic temperature. The CO abundance per unit velocity width was set to be 10^{-4} (km s^{-1} pc^{-1})$^{-1}$. (*d*) Same as (*c*), but at $Z(CO)/(dv/dr) = 10^{-5}$ (km s^{-1} pc^{-1})$^{-1}$.

Galaxy shows that $R_{13/12}$ is nearly constant in the central parts of molecular clouds, whereas $R_{13/12}$ averaged over larger scales varies from place to place (L. Bronfman 1996, private communication). This result supports the adoptability of the two-component model. Provided that molecular gas is composed of two components with respect to $R_{13/12}$—dense gas with $R_{13/12} = 1/3$ and tenuous gas with $R_{13/12} = 1/20$—we can extract the dense molecular gas fraction on the luminosity basis. The dense molecular gas fraction $f_{\rm dense}$ is given by the ratio of CO luminosity from dense molecular gas to the total CO luminosity as $f_{\rm dense} = (60R_{13/12} - 3)/17$. Provided that the CO-to-H_2 conversion factor is nearly independent of gas density near the density range 10^2–$10^{3.5}$ cm^{-3} as shown by Sakamoto (1996), this luminosity fraction reads the mass fraction of dense gas. This analysis yields a reasonable value of $f_{\rm dense} \simeq 1/2$ for Galactic giant molecular clouds with $R_{13/12} \simeq 1/5$.

5.1.3. *Effect of Cloud Overlapping*

Since NGC 891 is seen edge-on, one might wonder whether $R_{13/12}$ is sensitive to the cloud overlapping or not. According to Burton & Gordon (1978), who evaluated the degree of shadowing of one cloud by another, the shadowing is not prevalent in the (edge-on) Milky Way for molecular clouds probed by the ^{12}CO $J = 1$–0 emission. Namely, the assemblage of clouds is transparent even though individual clouds are opaque. We may be able to assume that virtually all molecular gas in NGC 891 is accessible to our observations. The observed line intensity ratio would thus faithfully reflect the physical conditions of molecular gas in the beam. This is also evident from Figure 5, which demonstrates that there is little, if any, systematic increase in $R_{13/12}$ toward the terminal velocity, where the effect of cloud overlapping is most severe.

5.2. *Properties of Molecular Gas in the Main Disk*

A quantitative inquiry into the physical properties of molecular gas is possible using the ratio of volume emissivities obtained in § 4. The radial distribution of the $^{13}CO/^{12}CO$ emissivity ratio plotted in Figure 6 provides evidence for a large-scale variation in the properties of molecular gas as a function of galactocentric distance. The $^{13}CO/^{12}CO$ emissivity ratio exhibits a notable peak of $\simeq 1/4.5$ near 4 kpc, and decreases systematically outward down to $\lesssim 1/10$ at 10 kpc. A similar systematic decreasing trend was also found for molecular gas in the Milky Way by means of the $^{13}CO/^{12}CO$ ratio (Liszt et al. 1984). The CO $J = 2$–1/$J = 1$–0 ratio (Handa et al. 1993; Sakamoto et al. 1995, 1996a), the HCN/CO ratio (Helfer & Blitz 1996), and the CS/CO ratio (Helfer & Blitz 1996) also exhibit the systematic outward decrease in the Milky Way. We may thus naturally expect that all these systematic variations in line ratios observed in the Milky Way have the same origin—a systematic decrease in gas density for increasing Galactocentric distance. Confinement of the bright ^{13}CO emission to a few cloud associations in Figure 4 supports the idea that a larger fraction of dense gas is the possible origin of the variation in $R_{13/12}$.

We plotted in Figure 8 the ratio of dense ($\gtrsim 1 \times 10^3$ cm^{-3}) gas to the total molecular gas calculated from the $^{13}CO/^{12}CO$ emissivity ratio in the manner described in § 5.1.2. Dense gas is the major form of interstellar gas from 2.5 to 6 kpc, and tenuous gas dominates the emission in the outer part ($\gtrsim 6$ kpc) of the galaxy. Since interstellar gas within 10 kpc from the center is mostly in molecular form (Sofue & Nakai 1993; Sofue, Honma, & Arimoto 1995), this large-scale variation in properties of molecular gas will be ascribed to compression of molecular gas with a strength dependent on galactocentric distance rather than dissociative stripping of low-density molecular gas. Larger pressure in the inner part of the galaxy provides a possible explanation for the radial variation in the fraction of dense gas.

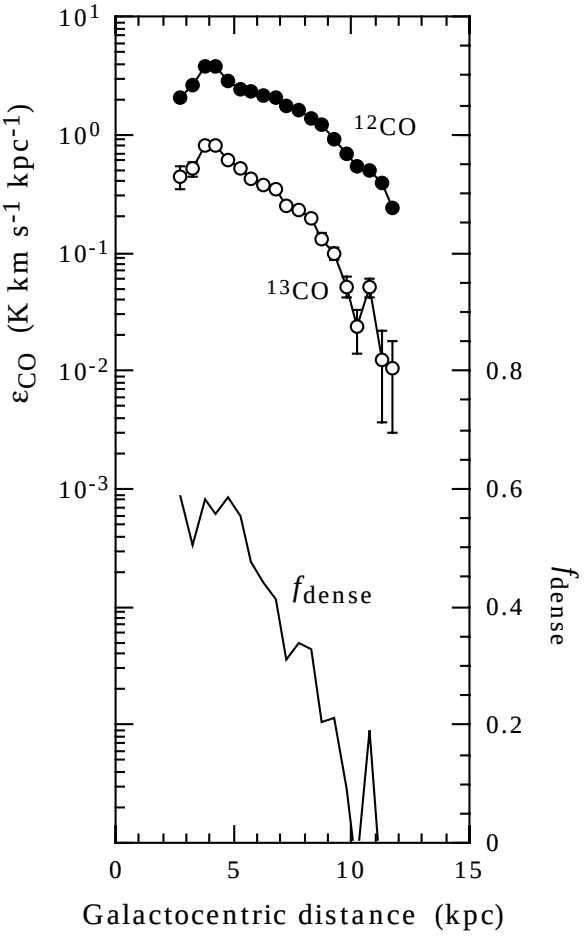

FIG. 8.—Volume emissivities of ^{12}CO $J = 1$–0 and ^{13}CO $J = 1$–0 emissions. Error bars represent 1 σ deviations. Ratio of dense ($\gtrsim 1 \times 10^3$ cm^{-3}) molecular gas to the total molecular gas as a function of galactocentric distance is also plotted. The ratio was calculated from the ratio of ^{13}CO to ^{12}CO emissivities in the manner described in the text.

5.3. *Properties of Molecular Gas in the Nuclear Disk*

The $^{13}CO/^{12}CO$ intensity ratio is $1/(15.4 \pm 6.0)$ in the nuclear disk of about 550 pc radius as we have seen in § 3. This value is not as high as we expect from the radial dependence of the ratio in the main disk. Why is the ratio so low in the nuclear disk?

Reasonable variations in the CO/H_2 abundance ratio and the $^{13}CO/^{12}CO$ isotope ratio only are insufficient to explain the observed variation in the $^{13}CO/^{12}CO$ intensity ratio, as we have already seen in § 5.1.1. We are left with a possible increase in gas kinetic temperature, a decrease in gas density, an unusually large velocity gradient, or an external heating source. We can test the reason for the suppressed $R_{13/12}$ in the central region through excitation analysis of the $J = 2$–1/$J = 1$–0 intensity ratio. According to the sensitive ^{12}CO $J = 1$–0 and $J = 2$–1 profiles toward the central region presented by García-Burillo & Guélin (1995) in their Figures 1 and 2, the $J = 2$–1/$J = 1$–0 intensity ratio is $\simeq 1.0$ in the nuclear disk. This high $J = 2$–1/$J = 1$–0 intensity ratio implies that most of the emitting gas is sufficiently warm and dense to excite the $J = 2$ level. It is thus most likely that the CO emission from the nuclear disk of NGC 891 is dominated by that from warm molecular gas ($\gtrsim 40$ K) with a moderate gas density ($\sim 10^3$ cm^{-3}) that is dense enough to excite both the $J = 1$–0 and $J = 2$–1 transitions of ^{12}CO but not to fully excite the $J = 1$–0 transition of ^{13}CO. Similar low values of $R_{13/12}$ are also reported in the central regions of starburst galaxies [$\simeq 1/(13 \pm 6)$; Aalto et al. 1995] and in mergers ($\simeq 1/30$; Casoli et al. 1992) with high values of the $J = 2$–1/$J = 1$–0 intensity ratio. These might also be attributed to warm molecular gas in the centers of starburst galaxies and mergers.

6. SUMMARY

Results of high-resolution simultaneous strip-scan observations of the edge-on galaxy NGC 891 in ^{12}CO and ^{13}CO emissions are presented. This data set with accurate relative calibrations of intensity scale and pointing was analyzed to examine radial variations in surface density and physical properties of molecular gas.

The distribution of the ^{13}CO emission mimics that of the ^{12}CO emission except for the following: (1) There is little emission inside 3 kpc from the center including the nuclear disk. The $^{13}CO/^{12}CO$ intensity ratio is $1/(15.4 \pm 6.0)$ in the nuclear disk of about 550 pc radius. (2) Asymmetry of the distribution of the main-disk emission is larger in the ^{13}CO emission. (3) Intense ^{13}CO emission in the main disk is confined to the inner edges of the molecular ring near 4 kpc and to a few discrete complexes. (4) The $^{13}CO/^{12}CO$ total luminosity ratio was 1/6.6. (5) The $^{13}CO/^{12}CO$ emissivity

ratio exhibits a notable peak of $\simeq 1/4.5$ near 4 kpc, and decreases systematically outward down to $\lesssim 1/10$ at 10 kpc. All these trends quantitatively agree with those found in the Milky Way.

The faintness of the nuclear disk in the ^{13}CO emission may better be attributed to the predominance of warm molecular gas of moderate density in this region. The low $^{13}CO/^{12}CO$ intensity ratio in starburst nuclei and mergers may have the same origin. The radial decrease in the $^{13}CO/^{12}CO$ ratio in the main disk can be interpreted in terms of radial decrease in the ratio of dense molecular gas to total molecular gas. Since interstellar gas in the inner part of the galaxy is mostly molecular, this large-scale variation in properties of molecular gas will be ascribed to compression of molecular gas with its strength dependent on galactocentric distance rather than dissociation of low-density molecular gas by UV photons from young stars in the inner part of the galaxy.

We are deeply indebted to the anonymous referee for helpful suggestions that clarified the manuscript. Thanks are due to Baltasar Vila-Vilaro for a critical reading of the manuscript, and to Franz Schöniger for his assistance during the observations. This work was carried out under the common-use observation program at the Nobeyama Radio Observatory (NRO). NRO, a branch of the National Astronomical Observatory, is a radio observing facility open to outside users. S. S. and M. H. were financially supported by the Japan Society for the Promotion of Science.

REFERENCES

Aalto, S., Booth, R. S., Black, J. H., & Johansson, L. E. B. 1995, A&A, 300, 369
Baldwin, J. E., & Pooley, G. G. 1973, MNRAS, 161, 127
Blitz, L., & Stark, A. A. 1986, ApJ, 300, L89
Bronfman, L., Bitran, M. E., & Thaddeus, P. 1988a, in Molecular Clouds in the Milky Way and External Galaxies, ed. R. L. Dickman, R. L. Snell, & J. S. Young (New York: Springer), 318
Bronfman, L., Cohen, R. S., Alvarez, H., May, J., & Thaddeus, P. 1988b, ApJ, 324, 248
Burton, W. B., & Gordon, M. A. 1978, A&A, 63, 7
Casoli, F., Dupraz, C., & Combes, F. 1992, A&A, 264, 55
Dame, T. M. 1993, in Back to the Galaxy, ed. S. S. Holt & F. Verter (New York: AIP), 267
Eckart, A., Downes, D., Genzel, R., Harris, A. I., Jaffe, D. T., & Wild, W. 1990, ApJ, 348, 434
García-Burillo, S., & Guélin, M. 1995, A&A, 299, 657
García-Burillo, S., Guélin, M., & Cernicharo, J. 1993, A&A, 274, 123
García-Burillo, S., Guélin, M., Cernicharo, J., & Dahlem, M. 1992, A&A, 266, 21
Handa, T., Hasegawa, T., Hayashi, M., Sakamoto, S., Oka, T., & Dame, T. M. 1993, in Back to the Galaxy, ed. S. S. Holt & F. Verter (New York: AIP), 315
Handa, T., Sofue, Y., Ikeuchi, S., Kawabe, R., & Ishizuki, S. 1992, PASJ, 44, L51
Helfer, T. T., & Blitz, L. 1997, ApJ, in press
Liszt, H. 1993, ApJ, 411, 720
Liszt, H. S. 1995, ApJ, 462, L163
Liszt, H. S., Burton, W. B., & Xiang, D. -L. 1984, A&A, 140, 303
Polk, K. S., Knapp, G. R., Stark, A. A., & Wilson, R. W. 1988, ApJ, 332, 432
Rickard, L. J, & Blitz, L. 1985, ApJ, 292, L57
Sakamoto, S. 1996, ApJ, 462, 215
Sakamoto, S., Hasegawa, T., Hayashi, M., Handa, T., & Oka, T. 1995, ApJS, 100, 125
———. 1996a, ApJ, submitted
Sakamoto, S., Hasegawa, T., Hayashi, M., Morino, J.-I., & Sato, K. 1996b, ApJ, submitted
Sakamoto, S., Hayashi, M., Hasegawa, T., Handa, T., & Oka, T. 1994, ApJ, 425, 641
Sancisi, R., & Allen, R. J. 1979, A&A, 74, 73
Sanders, D. B., Scoville, N. Z., Tilanus, R. P. J., Wang, Z., & Zhou, S. 1993, in Back to the Galaxy, ed. S. S. Holt & F. Verter (New York: AIP), 311
Sanders, D. B., Solomon, P. M., & Scoville, N. Z. 1984, ApJ, 276, 182
Scoville, N. Z., Thakkar, D., Carlstrom, J. E., & Sargent, A. I. 1993, ApJ, 404, L59
Sofue, Y., Honma, M., & Arimoto, N. 1995, A&A, 296, 33
Sofue, Y., & Nakai, N. 1993, PASJ, 45, 139
Sofue, Y., Nakai, N., & Handa, T. 1987, PASJ, 39, 47
Solomon, P. M. 1983, in Internal Kinematics and Dynamics of Galaxies, ed. E. Athanassoula (Dordrecht: Reidel), 35
Solomon, P. M., Scoville, N. Z., & Sanders, D. B. 1979, ApJ, 232, L89
Strong, A. W., et al. 1988, A&A, 207, 1
Wall, W. F., Jaffe, D. T., Bash, F. N., Israel, F. P., Maloney, P. R., & Baas, F. 1993, ApJ, 414, 98
Wiklind, T., Rydbeck, G., Hjalmarson, Å., & Bergman, P. 1990, A&A, 232, L11
Wilson, T. L., & Rood, R. T. 1994, ARA&A, 32, 191
Xie, S., Young, J., & Schloerb, P. F. 1994, ApJ, 421, 434